Inorg. Chem. **2004**, *43*, 2695–2702

Platinum–Rhodium Carbonyl Clusters: New Structures and New Types of Dynamical Activity

Richard D. Adams,* Burjor Captain, Perry J. Pellechia, and Jack L. Smith, Jr.

Department of Chemistry and Biochemistry and the USC Nanocenter, University of South Carolina, Columbia, South Carolina 29208

Received December 3, 2003

The reaction of $Rh_4(CO)_{12}$ with $Pt(PBu^t_3)_2$ in CH_2Cl_2 at room temperature yielded three new complexes: $Rh_4(CO)_4(\mu\text{-}CO)_4(\mu_4\text{-}CO)(PBu^t_3)_2[Pt(PBu^t_3)]$, **10**, $Rh_2(CO)_8[Pt(PBu^t_3)]_2[Pt(CO)]$, **11**, and $Rh_2(CO)_8[Pt(PBu^t_3)]_3$, **12**. The reaction of $Rh_4(CO)_{12}$ with an excess of $Pt(PBu^t_3)_2$ in hexane at 68 °C yielded the new hexarhodium–tetraplatinum compound, $Rh_6(CO)_{16}[Pt(PBu^t_3)]_4$, **13**, in a low yield. All four compounds were characterized by ^{31}P NMR and single-crystal X-ray diffraction analyses. Compound **10** contains an unsymmetrical quadruply bridging carbonyl ligand in the fold of a butterfly tetrahedral cluster of four rhodium atoms with a $Pt(PBu^t_3)$ group bridging the hinge of the butterfly tetrahedron. Compound **11** contains an unsaturated trigonal bipyramidal Rh_2Pt_3 cluster. Compound **12** is similar to **11** except the trigonal bipyramidal Rh_2Pt_3 cluster opened by cleavage of one Pt–Rh bond due to steric interactions produced by the replacement of one of the carbonyl ligands in **11** with a tri-*tert*-butylphosphine ligand. Compound **12** undergoes facile dynamical rearrangements of the metal atoms in the cluster which average the three inequivalent phosphine ligands on the platinum atoms. Compound **13** contains an octahedral cluster of six rhodium atoms with four $Pt(PBu^t_3)$ groups bridging edges of that octahedron.

Introduction

Mixed-metal (heteronuclear) molecular cluster complexes have attracted considerable interest because of their use as precursors for the preparation of heterogeneous catalysts on oxide supports.[1] Mixed-metal clusters have been found to be good precursors for the preparation of a variety of supported bimetallic nanoparticles.[1−6]

There have been major efforts to prepare bimetallic cluster complexes containing palladium[7] and platinum[8] in recent years. Recently, we have shown that the compounds $M(PBu^t_3)_2$, M = Pd and Pt, containing the sterically crowded tri-*tert*-butylphosphine ligand are excellent reagents for the addition of $M(PBu^t_3)$ groups to ruthenium−ruthenium bonds and ruthenium−platinum bonds to yield higher nuclearity mixed-metal cluster complexes containing palladium and platinum.[9] For example, $Pd(PBu^t_3)_2$ reacts with $Ru_3(CO)_{12}$ and $Ru_6(CO)_{17}(\mu_6\text{-}C)$ to yield the $Pd(PBu^t_3)$ adducts $Ru_3(CO)_{12}[Pd(PBu^t_3)]_3$, **1**, and $Ru_6(CO)_{17}(\mu_6\text{-}C)[Pd(PBu^t_3)]_2$, **2**, respectively.[9]

We have also prepared the adduct $Ru_5(CO)_{15}(C)[PtPBu^t_3]$, **3**, by the reaction of $Pt(PBu^t_3)_2$ with $Ru_5(CO)_{15}(\mu_5\text{-}C)$.[10,11] This compound in solution exists as a mixture of two isomers, a closed form, **3a**, and an open form, **3b**, that are

(1) (a) Thomas, J. M.; Johnson, B. F. G.; Raja, R.; Sankar, G.; Midgley, P. A. *Acc. Chem. Res.* **2003**, *36*, 20. (b) Raja, R.; Khimyak, T.; Thomas, J. M.; Hermans, S.; Johnson, B. F. G. *Angew. Chem., Int. Ed.* **2001**, *40*, 4638. (c) Hermans, S.; Raja, R.; Thomas, J. M.; Johnson, B. F. G.; Sankar, G.; Gleeson, D. *Angew. Chem., Int. Ed.* **2001**, *40*, 1211. (d) Raja, R.; Sankar, G.; Hermans, S.; Shephard, D. S.; Bromley, S.; Thomas, J. M.; Johnson, B. F. G.; Maschemeyer, T. *Chem. Commun.* **1999**, 1571. (e) Shephard, D. S.; Maschmeyer, T.; Johnson, B. F. G.; Thomas, J. M.; Sankar, G.; Ozkaya, D.; Zhou, W.; Oldroyd, R. D.; Bell, R. G. *Angew. Chem., Int. Ed. Engl.* **1997**, *36*, 2242. (f) Raja, R.; Sankar, G.; Hermans, S.; Shephard, D. S.; Bromley, S.; Thomas, J. M.; Johnson, B. F. G. *Chem. Commun.* **1999**, 1571. (g) Shephard, D. S.; Maschmeyer, T.; Sankar, G.; Thomas, J. M.; Ozkaya, D.; Johnson, B. F. G.; Raja, R.; Oldroyd, R. D.; Bell, R. G. *Chem. Eur. J.* **1998**, *4*, 1214.
(2) Toshima, N.; Yonezawa, T. *New J. Chem.* **1998**, 1179.
(3) Johnson, B. F. G. *Coord. Chem. Rev.* **1999**, *192*, 1269.
(4) Midgley, P. A.; Weyland, M.; Thomas, J. M.; Johnson, B. F. G. *Chem. Commun.* **2001**, 907.
(5) Nashner, M. S.; Frenkel, A. I.; Somerville, D.; Hills, C. W.; Shapley, J. R.; Nuzzo, R. G. *J. Am. Chem. Soc.* **1998**, *120*, 8093.
(6) Nashner, M. S.; Frenkel, A. I.; Adler, D. L.; Shapley, J. R.; Nuzzo, R. G. *J. Am. Chem. Soc.* **1997**, *119*, 7760.
(7) Lee, S.-M.; Wong, W.-T. *J. Cluster Sci.* **1998**, *9*, 417.
(8) (a) Farrugia, L. J. *Adv. Organomet. Chem.* **1990**, *31*, 301. (b) Pignolet, L. H.; Aubart, M. A.; Craighead, K. L.; Gould, R. A. T.; Krogstad, D. A.; Wiley, J. S. *Coord. Chem. Rev.* **1995**, *143*, 219. (c) Xiao, J. L.; Puddephatt, R. J. *Coord. Chem. Rev.* **1995**, *143*, 457.
(9) Adams, R. D.; Captain, B.; Fu, W.; Smith, M. D. *J. Am. Chem.* Soc. **2002**, *124*, 5628.
(10) Adams, R. D.; Captain, B.; Fu, W.; Pellechia, P. J.; Smith, M. D. *Angew. Chem., Int. Ed.* **2002**, *41*, 1951.
(11) Adams, R. D.; Captain, B.; Fu, W.; Pellechia, P. J.; Smith, M. D. *Inorg. Chem.* **2003**, *42*, 2094.

10.1021/ic0353920 CCC: $27.50
Published on Web 03/17/2004

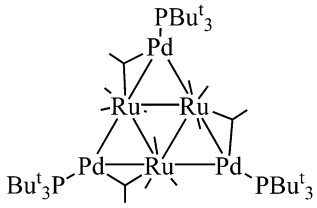

1

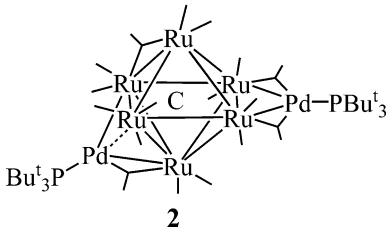

2

in rapid equilibrium on the NMR time scale at room temperature. Similarly, $Pd(PBu^t_3)_2$ also reacts with $Ru_5(CO)_{15}(\mu_5\text{-C})$ to produce the palladium compounds $Ru_5(CO)_{15}(\mu_6\text{-C})[Pd(PBu^t_3)]_n$ where $n = 1$ (**4**) and $n = 2$ (**5**), which also exhibit similar dynamic behavior of their metal cluster cores in solution.[11]

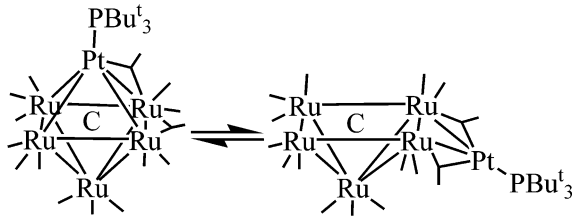

3a **3b**

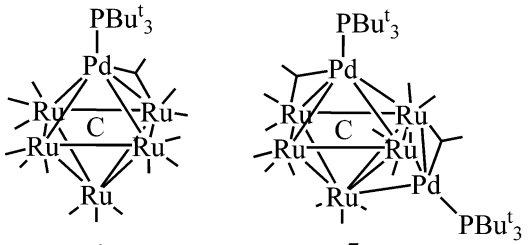

4 **5**

In addition, we have also shown that $Pt(PBu^t_3)$ and $Pd(PBu^t_3)$ groups add across the Ru−Pt bonds in the mixed-metal cluster $PtRu_5(CO)_{16}(\mu_6\text{-C})$ to afford the adducts $PtRu_5(CO)_{16}(\mu_6\text{-C})[M(PBu^t_3)]_n$, **6** and **7,** where M = Pt and $n = 1$ or $n = 2$, respectively, and **8** and **9**, where M = Pd and $n = 1$ or $n = 2$, respectively.[12]

Platinum−rhodium catalysts form the basis for the modern three-way automotive catalytic converter.[13] To test the ability of the $Pt(PBu^t_3)$ group to add to the metal−metal bonds of other transition elements, we have now investigated the reaction of $Pt(PBu^t_3)_2$ with the tetrarhodium cluster $Rh_4(CO)_{12}$. Four products: a tetrarhodium−platinum compound $Rh_4(CO)_4(\mu\text{-CO})_4(\mu_4\text{-CO})(PBu^t_3)_2[Pt(PBu^t_3)]$, **10,** two dirhodium−platinum compounds $Rh_2(CO)_8[Pt(PBu^t_3)]_2[Pt(CO)]$, **11**, $Rh_2(CO)_8[Pt(PBu^t_3)]_3$, **12**, and a hexarhodium-tetraplatinum cluster, $Rh_6(CO)_{16}[Pt(PBu^t_3)]_4$, **13**, were obtained from this reaction. The synthesis and structural characterizations of these compounds are reported herein including studies of dynamics of the metal clusters exhibited by these compounds in solution by NMR spectroscopy.

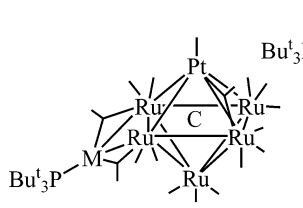

6 M = Pt
8 M = Pd

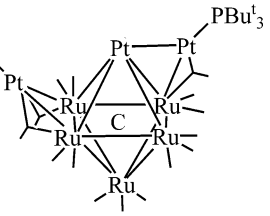

7

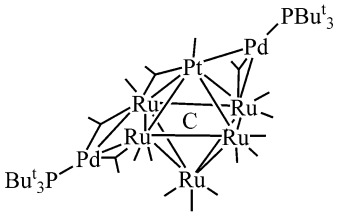

9

Experimental Section

General Data. All reactions were performed under a nitrogen atmosphere. Reagent-grade solvents were dried by the standard procedures and were freshly distilled prior to use. Infrared spectra were recorded on a Thermo-Nicolet Avatar 360 FT-IR spectrophotometer. ^{1}H NMR spectra were recorded on a Mercury 300 and a Varian Inova spectrometer operating at 300.1 and 400.1 MHz. ^{31}P{^{1}H} NMR spectra were recorded on a Mercury 300 and a Varian Inova 400 and 500 spectrometer operating at 121.5, 161.9, and 202.5 MHz, respectively. ^{31}P NMR spectra were externally referenced against 85% *o*-H_3PO_4. Elemental analyses were performed by Desert Analytics (Tucson, AZ). Product separations were performed by TLC in air on Analtech 0.5-mm silica gel 60-Å F_{254} glass plates. $Rh_4(CO)_{12}$ and $Pt(PBu^t_3)_2$ were obtained from Strem and were used without further purification.

Reaction of $Rh_4(CO)_{12}$ with $Pt(PBu^t_3)_2$. $Pt(PBu^t_3)_2$ (22.4 mg, 0.037 mmol) was added to a solution of $Rh_4(CO)_{12}$ (28.0 mg, 0.037 mmol) in 25 mL of CH_2Cl_2. The color of the solution immediately turned from bright red to brown. The reaction mixture was then stirred at room temperature for an additional 10 min, after which the solvent was removed in vacuo. The products were separated by TLC using a 3:2 hexane/methylene chloride solvent mixture to yield in order of elution: 7.7 mg (14%) of $Rh_2(CO)_8[Pt(PBu^t_3)]_2[Pt(CO)]$, **11**; 4.0 mg (7%) of $Rh_4(CO)_4(\mu\text{-CO})_4(\mu_4\text{-CO})(PBu^t_3)_2[Pt(PBu^t_3)]$, **10**, and 13.1 mg (22%) of $Rh_2(CO)_8[Pt(PBu^t_3)]_3$, **12**. Spectral data for **10**: IR ν_{CO} (cm^{-1} in CH_2Cl_2): 2004 (vs), 1900 (m), 1871 (m), 1846 (s), 1827 (m, sh), 1704 (w, br). ^{1}H NMR (CD_2Cl_2 in ppm): $\delta = 1.42$ (d, 54 H, CH_3, $^3J_{P-H} = 13$ Hz), 1.40 (d, 27 H, CH_3, $^3J_{P-H} = 13$ Hz). ^{31}P{^{1}H} NMR (CD_2Cl_2 in ppm): $\delta =$ 89.8 (tt, 1P, $^1J_{Pt-P} = 4946$ Hz, $^2J_{Rh-P} = 13$ Hz, $^3J_{Rh-P} = 3$ Hz), 86.4 (d, 2P, $^1J_{Rh-P} = 236$ Hz). Anal. Calcd: C, 36.87; H, 5.57. Found: C, 36.48; H, 5.67. Spectral data for **11**: IR ν_{CO} (cm^{-1} in hexane): 2075 (w), 2069 (w), 2064 (m), 2058 (w), 2041 (w), 2032 (s), 2017 (vs), 1873 (m), 1851 (m). ^{1}H NMR ($CDCl_3$ in ppm): δ = 1.26 (d, 54 H, CH_3, $^3J_{P-H} = 13$ Hz). ^{31}P{^{1}H} NMR ($CDCl_3$ in

(12) Adams, R. D.; Captain, B.; Fu, W.; Smith, M. D. *J. Organomet. Chem.* **2003**, *682*, 113.
(13) (a) Oh, S. H.; Carpenter, J. E. *J. Catal.* **1986**, *98*, 178. (b) Barbier, J., Jr.; Duprez, D. *Appl. Catal., B* **1994**, *4*, 105.

Table 1. Crystallographic Data for Compounds **10**, **11**, **12**, and **13**

compound	**10**	**11**	**12**	**13**
empirical formula	$Pt_1Rh_4P_3O_9C_{45}H_{81}$	$Pt_3Rh_2P_2O_9C_{33}H_{54}$	$Pt_3Rh_2P_3O_8C_{44}H_{81}$	$Pt_4Rh_6P_4O_{16}C_{64}H_{108}\cdot 2CH_2Cl_2$
fw	1465.74	1447.79	1622.09	2825.06
cryst syst	orthorhombic	monoclinic	orthorhombic	monoclinic
lattice params				
a (Å)	23.1623(9)	12.8419(5)	39.314(3)	25.3187(15)
b (Å)	12.6080(5)	20.2154(8)	12.0693(9)	14.6823(9)
c (Å)	37.4151(15)	16.5434(7)	12.3772(9)	26.4675(16)
α (deg)	90	90	90	90
β (deg)	90	91.277(1)	90	112.726(1)
γ (deg)	90	90	90	90
V (Å^3)	10926.3(7)	4293.7(3)	5872.9(7)	9075.1(9)
space group	*Pbca* (No. 61)	$P2_1/n$ (No. 14)	$Pna2_1$ (No. 33)	$C2/c$
Z value	8	4	4	4
ρ_{calc} (g/cm^3)	1.782	2.240	1.835	2.068
μ (Mo Kα) (mm^{-1})	3.870	10.612	7.794	7.442
temp (K)	296(2)	296(2)	296(2)	296(2)
$2\Theta_{max}$ (deg)	56.64	56.62	52.04	50.06
no. obs. ($I > 2\sigma(I)$)	10540	7419	8834	6880
no. params	586	460	565	437
GOF	1.067	1.026	1.020	1.062
max. shift in cycle	0.003	0.001	0.007	0.008
residuals[a]: R1; wR2	0.0331; 0.0770	0.0468; 0.1151	0.0487; 0.0916	0.0496; 0.1321
abs correction,	SADABS	SADABS	SADABS	SADABS
max/min	1.000/0.662	1.000/0.512	1.000/0.699	1.00; 0.395
largest peak in final diff. map (e$^-$/Å^3)	1.886	4.202	1.179	2.424

[a] $R = \sum_{hkl}(||F_{obs}| - |F_{calc}||)/\sum_{hkl}|F_{obs}|$; $R_w = [\sum_{hkl}w(|F_{obs}| - |F_{calc}|)^2/\sum_{hkl}wF_{obs}^2]^{1/2}$, $w = 1/\sigma^2(F_{obs})$; GOF $= [\sum_{hkl}w(|F_{obs}| - |F_{calc}|)^2/(n_{data} - n_{vari})]^{1/2}$.

ppm): $\delta = 96.3$ (t, 2P, $^1J_{Pt-P} = 5432$ Hz, $^2J_{Pt-P} = 133$ Hz, $^2J_{Rh-P} = 12$ Hz). Anal. Calcd: C, 27.38; H, 3.76. Found: C, 27.63; H, 3.94. Spectral data for **12**: IR ν_{CO} (cm^{-1} in hexane): 2081 (vw), 2075 (vw), 2069 (w), 2065 (w), 2059 (w), 2041 (w), 2029 (s), 2000 (vs), 1851 (m), 1823 (s), 1802 (m). ^{1}H NMR (CD_2Cl_2 in ppm): $\delta = 1.33$ (d, 81 H, CH_3, $^3J_{P-H} = 13$ Hz). ^{31}P{^{1}H} NMR (d_8-toluene at −80 °C in ppm): $\delta = 112.2$ (s, 1P, $^1J_{Pt-P} = 6257$ Hz), 85.5 (s, 1P, $^1J_{Pt-P} = 4875$ Hz), 78.5 (s, 1P, $^1J_{Pt-P} = 5176$ Hz). Anal. Calcd: C, 32.58; H, 5.03. Found: C, 31.14; H, 4.91.

Synthesis of $Rh_6(CO)_{16}[Pt(PBu^t_3)]_4$, 13. $Pt(PBu^t_3)_2$ (65.3 mg, 0.11 mmol) was added to a solution of $Rh_4(CO)_{12}$ (23.1 mg, 0.031 mmol) in hexane solvent (25 mL). The mixture was then heated to reflux and stirred for 10 min. After cooling, the solvent was removed in vacuo, and the products were then separated by TLC using a 3:2 hexane/methylene chloride solvent mixture to yield 7.2 mg of a brown band. The ^{31}P{^{1}H} NMR spectrum of the brown band showed two resonances in a 1:1 ratio. The brown band was then dissolved in 3 mL of CH_2Cl_2 to which $Pt(PBu^t_3)_2$ (4 mg, ∼4 equiv) was added. Five milligrams of the brown band was again separated by TLC by using a 3:2 hexane/methylene chloride solvent mixture. The product $Rh_6(CO)_{16}[Pt(PBu^t_3)]_4$, **13**, was finally isolated in a pure form in 3% yield (2.8 mg) by recrystallization of this brown band at 8 °C by slow evaporation of solvent from a solution in a hexane/methylene chloride solvent mixture. Spectral data for **13**: IR ν_{CO} (cm^{-1} in CH_2Cl_2): 2016 (vs), 1852 (s), 1840 (s), 1826 (m), 1740 (w). ^{1}H NMR (CD_2Cl_2 in ppm): $\delta = 1.46$ (d, 108 H, CH_3, $^3J_{P-H} = 13$ Hz). ^{31}P{^{1}H} NMR (CH_2Cl_2 in ppm): $\delta = 98.4$ (septet, 4P, $^1J_{Pt-P} = 5977$ Hz, $^2J_{P-Rh} = 3$ Hz). Anal. Calcd: C, 28.93; H, 4.07. Found: C, 29.10; H, 4.34. NOTE: The second product in the original brown band could not be isolated in a pure form and could not be fully characterized.

Crystallographic Analyses. Dark red single crystals of **10**, **11**, and **12** suitable for X-ray diffraction analyses were obtained by slow evaporation of solvent from solutions in hexane/methylene chloride solvent mixtures at −25 °C. Dark red single crystals of **13** were obtained by slow evaporation of the same solvent mixture at 8 °C. Each data crystal was glued onto the end of a thin glass fiber. X-ray intensity data were measured by using a Bruker SMART APEX CCD-based diffractometer using Mo Kα radiation ($\lambda = 0.71073$ Å). The raw data frames were integrated with the SAINT+ program by using a narrow-frame integration algorithm.[14] Correction for Lorentz and polarization effects were also applied with SAINT+. An empirical absorption correction based on the multiple measurement of equivalent reflections was applied using the program SADABS. Both structures were solved by a combination of direct methods and difference Fourier syntheses and refined by full-matrix least-squares on F^2, using the SHELXTL software package.[15] All non-hydrogen atoms were refined with anisotropic displacement parameters. Hydrogen atoms were placed in geometrically idealized positions and included as standard riding atoms during the least-squares refinements. Crystal data, data collection parameters, and results of the analyses are listed in Table 1.

Compounds **11** and **13** crystallized in the monoclinic crystal system. For compound **11** systematic absences in the intensity data confirmed the space group $P2_1/n$. The structure was solved and suitably refined in this space group. For compound **13** the space groups *Cc* and *C2/c* were indicated by the systematic absences in the data. The latter space group was chosen and confirmed by the solution and refinement of the structure. Crystallographically, this molecule lies on a C_2 symmetry site in the asymmetric unit. Compounds **10** and **12** crystallized in the orthorhombic crystal system. Systematic absences in the intensity data for compound **10** were consistent with the unique space group *Pbca*. For compound **12** the systematic absences in the data were consistent with the two space groups $Pna2_1$ and *Pnma*. The former space group was chosen and confirmed by the successful solution and refinement of the structure. Efforts to solve in the space group *Pnma* were unsuccessful.

NMR Calculations. Line shape analyses were performed on a Gateway PC by using the program EXCHANGE written by R. E. D. McClung of the Department of Chemistry, University of Alberta, Edmonton, Alberta, Canada. For compound **12** exchange rates were

(14) *SAINT+*, Version 6.2a; Bruker Analytical X-ray System, Inc.: Madison, WI, 2001.
(15) Sheldrick, G. M. *SHELXTL*, Version 6.1; Bruker Analytical X-ray Systems, Inc.: Madison, WI, 1997.

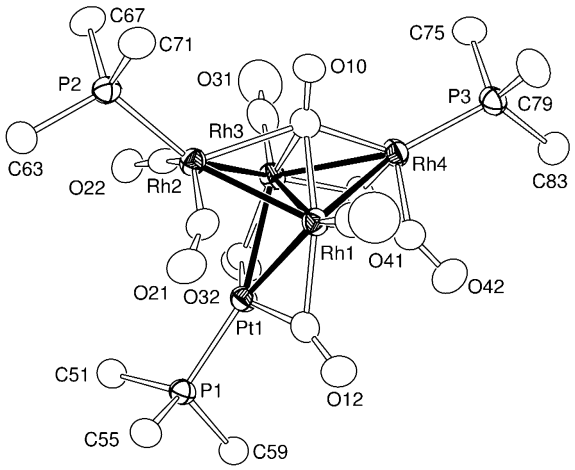

Figure 1. ORTEP diagram of the molecular structure of $Rh_4(CO)_4(\mu\text{-}CO)_4(\mu_4\text{-}CO)(PBu^t_3)_2[Pt(PBu^t_3)]$, **10**, showing 40% probability thermal ellipsoids. The methyl groups have been omitted for clarity.

determined at 11 different temperatures in the temperature range −90 to −15 °C. The activation parameters were determined from a least-squares fit of an Eyring plot (ln [hk/K_BT] vs $1/T$) using the program Microsoft Excel 97. Activation parameters for the exchange process between resonances at $\delta = 112.2$ and 85.5 are $\Delta H^{\ddagger} = 8.2(2)$ kcal mol^{-1}, $\Delta S^{\ddagger} = -2(1)$ cal mol^{-1} K^{-1}, and $\Delta G_{258}{}^{\ddagger} = 8.7(5)$ kcal mol^{-1}. Activation parameters for the exchange process of the resonance at $\delta = 78.5$ with the resonances at $\delta = 112.2$ and 85.5 are $\Delta H^{\ddagger} = 8.2(3)$ kcal mol^{-1}, $\Delta S^{\ddagger} = -3(1)$ cal mol^{-1} K^{-1}, and $\Delta G_{258}{}^{\ddagger} = 8.9(6)$ kcal mol^{-1}.

Results and Discussion

The reaction of $Rh_4(CO)_{12}$ with an equimolar amount of $Pt(PBu^t_3)_2$ at room temperature afforded three new complexes: $Rh_4(CO)_4(\mu\text{-}CO)_4(\mu_4\text{-}CO)(PBu^t_3)_2[Pt(PBu^t_3)]$, **10**, in 7% yield, $Rh_2(CO)_8[Pt(PBu^t_3)]_2[Pt(CO)]$, **11**, in 14% yield, and $Rh_2(CO)_8[Pt(PBu^t_3)]_3$, **12**, in 22% yield. All three compounds were characterized by a combination of IR, ^{1}H and ^{31}P NMR, and single-crystal X-ray diffraction analyses.

An ORTEP diagram of the molecular structure of compound **10** is shown in Figure 1. Selected interatomic distances and angles are listed in Table 2. The four rhodium atoms in this compound are arranged in the "butterfly" tetrahedral structure. The platinum atom of the $Pt(PBu^t_3)$ group bridges the Rh1−Rh3 "hinge" bond of the butterfly. The Rh−Rh bond distances lie in the range 2.7279(5)−2.7836(5) Å and are similar to those found in $Rh_4(CO)_{12}$, range 2.6603(17)−2.7642(12) Å.[16] There is an unsymmetrical quadruply bridging carbonyl ligand C10−O10 in the fold of the Rh_4 cluster. One of the Rh−C bonds, Rh2−C10 = 2.439(5) Å, is significantly longer than the other three: Rh1−C10 = 2.136(5), Rh3−C10 = 2.179(4), and Rh4−C10 = 2.195(5). This can be attributed to the higher coordination number at Rh2, which has two terminal (or weak semibridging) CO ligands plus one PBu^t_3 compared to the other rhodium atoms, which have one PBu^t_3 ligand and two bridging carbonyls (Rh4) or one terminal CO and two bridging COs (Rh1 and Rh3). The C10−O10 distance, 1.168(5) Å, is not much longer than that of a terminal carbonyl ligand, but the CO stretching frequency, observed as a broad absorption in the IR spectrum at 1704 cm^{-1}, is significantly lower than that found for terminal CO ligands. There are very few reported examples of similar quadruply bridging CO ligands in the literature. One was found in the compound $Cp_4Mo_2Ni_2S_2(\mu_4\text{-}CO)$.[17] In this compound the C−O bond distance is 1.18 Å and the CO stretching frequency was reported to be at 1653 cm^{-1}. The platinum atom is not symmetrically disposed with respect to the wing-tip rhodium atoms, Pt1···Rh2 = 3.3290(4) Å and Pt1···Rh4 = 4.4037(4) Å. This may be due to steric effects caused by the edge-bridging CO ligands on the two Rh−Rh bonds to Rh4.

The ^{31}P{^{1}H} NMR spectrum of **10** at room temperature shows two resonances in a 1:2 ratio, indicating that phosphine ligands on Rh2 and Rh4 are equivalent in solution or the molecule is undergoing a dynamical averaging process. Since the IR spectrum in solution is consistent with the structure found in the solid state, the latter explanation seems to be the more likely one. A rearrangement involving a rocking back and forth of the $Pt(PBu^t_3)$ group on the Rh1−Rh3 hinge bond accompanied by appropriate shifts of the CO ligands on Rh2 and Rh4 would average the two PBu^t_3 ligands on the rhodium atoms, eq 1.

Unfortunately, efforts to confirm the dynamics by variable temperature ^{31}P NMR spectroscopy to −55 °C showed no evidence for slowing of the process on the NMR time scale. The resonance at $\delta = 89.8$ corresponds to the PBu^t_3 group

Table 2. Selected Intramolecular Distances and Angles for Compounds **10** and **13**[a]

(a) Distances

compound **10**		compound **13**	
atoms	distance (Å)	atoms	distance (Å)
Pt(1)−Rh(1)	2.7630(4)	Pt(1)−Rh(1)	2.7210(4)
Pt(1)−Rh(3)	2.7727(4)	Pt(1)−Rh(3)	2.7353(7)
Pt(1)−P(1)	2.3667(10)	Pt(2)−Rh(2)	2.7364(7)
Rh(1)−Rh(2)	2.7506(5)	Pt(2)−Rh(4)	2.7113(4)
Rh(1)−Rh(3)	2.7836(5)	Rh(1)−Rh(2)	2.8070(9)
Rh(1)−Rh(4)	2.7594(5)	Rh(1)−Rh(3)	2.7616(9)
Rh(2)−Rh(3)	2.7279(5)	Rh(2)−Rh(3)	2.7826(10)
Rh(2)−P(2)	2.3749(12)	Rh(2)−Rh(4)	2.7573(9)
Rh(3)−Rh(4)	2.7358(5)	Rh(3)−Rh(4)	2.8071(9)
Rh(4)−P(3)	2.3681(11)		
Pt(1)···Rh(2)	3.3290(4)		
Pt(1)···Rh(4)	4.4037(4)		
Rh(2)···Rh(4)	4.3804(5)		
Rh(1)−C(10)	2.136(5)		
Rh(2)−C(10)	2.439(5)		
Rh(3)−C(10)	2.179(4)		
Rh(4)−C(10)	2.195(5)		
C(10)−O(10)	1.168(5)		

(b) Angles

compound **10**		compound **13**	
atoms	angle (deg)	atoms	angle (deg)
Rh(2)−Rh(1)−Rh(4)	105.307(15)	Rh(1)−Pt(1)−Rh(3)	60.81(2)
Rh(2)−Rh(1)−Pt(1)	74.280(11)	Rh(2)−Pt(2)−Rh(4)	60.81(2)
Rh(4)−Rh(1)−Pt(1)	105.769(13)	Rh(1)−Rh(2)−Rh(4)	90.17(3)
Rh(3)−Rh(2)−Rh(1)	61.071(12)		
Rh(1)−Pt(1)−Rh(3)	60.376(10)		

[a] Estimated standard deviations in the least significant figure are given in parentheses.

(16) Farrugia, L. J. *J. Cluster Sci.* **2000**, *11*, 39.

(17) Ping, L.; Curtis, M. D. *J. Am. Chem. Soc.* **1989**, *111*, 8279.

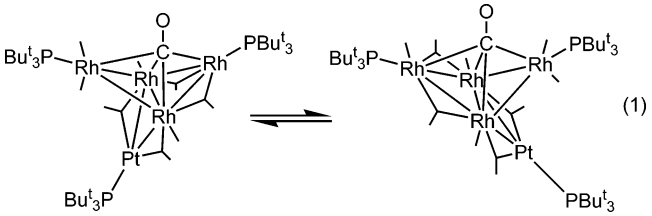

(1)

on the platinum atom and shows large one-bond coupling to platinum, $^1J_{Pt-P} = 4946$ Hz (^{195}Pt, spin $^1/_2$, 33% natural abundance). Furthermore, this resonance is split into a triplet of triplets with couplings of 13 and 3 Hz due to two-bond coupling to Rh1 and Rh3 and three-bond coupling to Rh2 and Rh4, respectively (^{103}Rh, spin $^1/_2$, 100% natural abundance). The ^{31}P resonance at $\delta = 86.4$ corresponds to the PBu^t_3 group on Rh2 and Rh4. This resonance is a doublet due to one-bond coupling to rhodium, $^1J_{Rh-P} \approx 236$ Hz. However, each of these resonances is further split due to the complex $AA'MM'X_2$ spin system that occurs due to the magnetic nonequivalence of Rh2 and Rh4. The measured line spacings of these resonances are not necessarily coupling constants and no effort to simulate these patterns was attempted.

The molecular structure of **11** is shown in Figure 2. Selected bond distances and angles are listed in Table 3. The structure of **11** consists of a trigonal bipyramidal cluster of two rhodium atoms and three platinum atoms. The equatorial triangle contains the rhodium atoms, Rh1 and Rh2, and one platinum atom, Pt3. The two apical positions are occupied by two platinum atoms, Pt1 and Pt2. A PBu^t_3 ligand is coordinated to each of the apical platinum atoms, Pt1 and Pt2, while the third platinum atom Pt3 contains a terminal CO ligand. The structure of the cluster of **11** is similar to that of the related compound $Rh_2Pt_3(CO)_9(PPh_3)_3$, **14**, that was obtained in a similar manner from the reaction of $Rh_4(CO)_{12}$ with $Pt(PPh_3)_3$,[18] except that **11** has one less ligand than **14**; that is, compound **11** has only 11 ligands (9 CO ligands and two phosphines) while **14** has 12 ligands (9 CO ligands and three phosphines). In particular, the platinum Pt2 has one phosphine and one terminal CO ligand in **14**, but the corresponding platinum atom in **11** has only the one PBu^t_3 ligand.

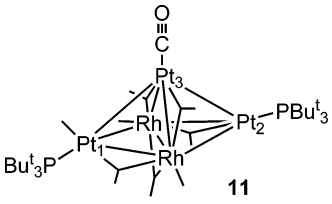

11

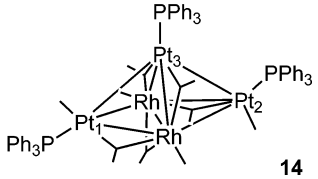

14

Accordingly, **11** has two less valence electrons than **14**, 70 cluster valence electrons for **11** versus 72 cluster valence electrons (as expected according to the cluster electron counting rules) for **14**. Thus, compound **11** is formally electron-deficient by the amount of two electrons, although

(18) Dolgushin, F. M.; Grachova, E. V.; Heaton, B. T.; Iggo, J. A.; Koshevoy, I. O.; Podkorytov, I. S.; Smawfield, D. J.; Tunik, S. P.; Whyman, R.; Yanovskii, A. I. *J. Chem. Soc., Dalton Trans.* **1999**, 1609.

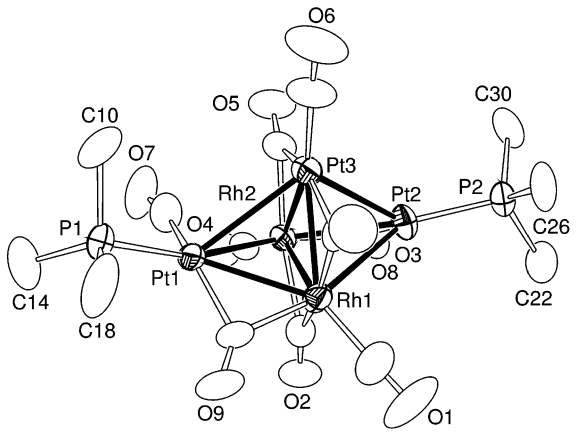

Figure 2. ORTEP diagram of the molecular structure of $Rh_2(CO)_8[Pt(PBu^t_3)]_2[Pt(CO)]$, **11**, showing 40% probability thermal ellipsoids. The methyl groups have been omitted for clarity.

Table 3. Selected Intramolecular Distances and Angles for Compounds **11** and **12**[a]

(c) Distances

compound **11**		compound **12**	
atoms	distance (Å)	atoms	distance (Å)
Pt(1)−Rh(1)	2.8138(7)	Pt(1)−Rh(1)	2.7008(11)
Pt(1)−Rh(2)	2.8820(7)	Pt(1)−Rh(2)	2.8877(10)
Pt(1)−Pt(3)	3.0622(5)	Pt(1)−Pt(3)	3.436(1)
Pt(1)−P(1)	2.365(2)	Pt(1)−P(1)	2.358(3)
Pt(2)−Rh(1)	2.9521(7)	Pt(2)−Rh(1)	2.7821(10)
Pt(2)−Rh(2)	2.8003(7)	Pt(2)−Rh(2)	2.8490(11)
Pt(2)−Pt(3)	2.8384(5)	Pt(2)−Pt(3)	3.0953(8)
Pt(2)−P(2)	2.280(2)	Pt(2)−P(2)	2.289(4)
Pt(3)−Rh(1)	2.7146(8)	Pt(3)−Rh(1)	2.7476(11)
Pt(3)−Rh(2)	2.6860(7)	Pt(3)−Rh(2)	2.7190(12)
Rh(1)−Rh(2)	2.6842(9)	Rh(1)−Rh(2)	2.7208(13)
		Pt(3)−P(3)	2.336(4)

(d) Angles

compound **11**		compound **12**	
atoms	angle (deg)	atoms	angle (deg)
Rh(1)−Pt(2)−Rh(2)	55.56(2)	Rh(1)−Pt(2)−Rh(2)	57.77(3)
Pt(3)−Pt(2)−Rh(1)	55.873(16)	Pt(3)−Pt(2)−Rh(1)	55.43(2)
Pt(1)−Rh(1)−Pt(2)	115.32(2)	Pt(1)−Rh(1)−Pt(2)	125.95(4)
Rh(2)−Pt(3)−Rh(1)	59.60(2)	Rh(2)−Pt(3)−Rh(1)	59.69(3)

[a] Estimated standard deviations in the least significant figure are given in parentheses.

platinum-containing trigonal bipyramidal clusters containing 70 electrons have been observed previously.[8] Comparison of the structures of **11** and **14** support the notion of electron deficiency. For example, compound **11** has one unusually short Pt−Pt bond distance, Pt2−Pt3 = 2.8384(5) Å and one normal Pt−Pt bond, Pt1−Pt3 = 3.0622(5) Å. The Pt−Pt bonds in **14** are both normal, 2.992(1) and 3.011(1) Å.[16] The short distance in **11** involves the metal atom Pt2, which has one less terminal CO ligand than that in **14**. The reason that **11** has fewer ligands than **14** may be due to the great steric bulk of the PBu^t_3 ligands in **11** compared to the smaller PPh_3 ligands in **14**. The Pt−Rh distances in **11** are comparable to those in **14**.

The $^{31}P\{^1H\}$ NMR spectrum of **11** shows a single resonance at 96.3 ppm, indicating that the two PBu^t_3 ligands are equivalent. This is not consistent with the solid-state structure, but could be explained by an averaging process

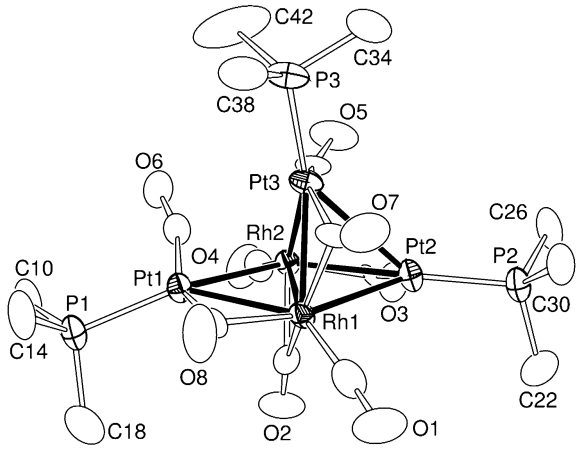

Figure 3. ORTEP diagram of the molecular structure of $Rh_2(CO)_8[Pt(PBu^t_3)]_3$, **12**, showing 40% probability thermal ellipsoids. The methyl groups have been omitted for clarity.

involving shifting of the CO ligands about the metal atoms, eq 2, such that the atoms Pt1 and Pt2 are interchanged. Attempts to resolve the separate resonances for the two phosphine ligands by NMR spectroscopy at −80 °C were unsuccessful. Rapid shifts of CO ligands on the NMR time scale for related Pt−Rh clusters have been observed previously. The averaged ^{31}P NMR resonance also exhibits fine structure due to couplings to the magnetically active metal atoms in the cluster, $^1J_{Pt-P} = 5432$ Hz, $^2J_{Pt-P} = 133$ Hz, and $^2J_{Rh-P} = 12$ Hz, which is consistent with the structure as found in the solid state.

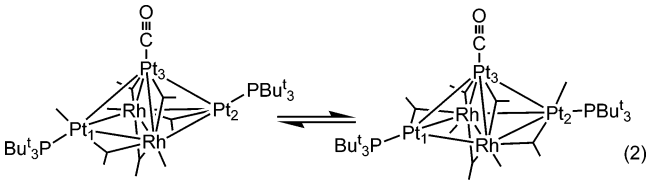

An ORTEP diagram of the molecular structure of **12** is shown in Figure 3. Selected bond distances and angles are listed in Table 3. Compound **12** is very similar to compound **11**, except that the CO ligand on Pt3 in **11** has been replaced by a PBu^t_3 ligand. Because of the increase in steric bulk at Pt3 caused by the PBu^t_3 ligand, the Pt1−Pt3 distance has become much longer than that in **11**, 3.436(1) vs 3.0622(5) Å in **11**.

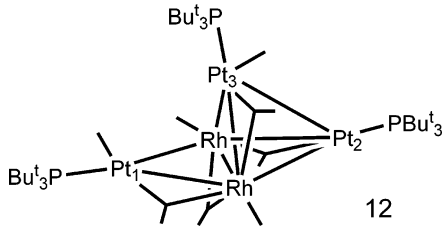

12

There is little or no bonding between these two atoms at this distance. The Pt2−Pt3 distance is also longer than that in **11**, 3.0953(1) vs 2.8384(5) Å, but is still short enough to imply the presence of significant direct Pt−Pt bonding. The Pt2−Pt3 distance in **14** is 2.992(1) Å. The increase in the Pt2−Pt3 distance in **12** may also be a consequence of the

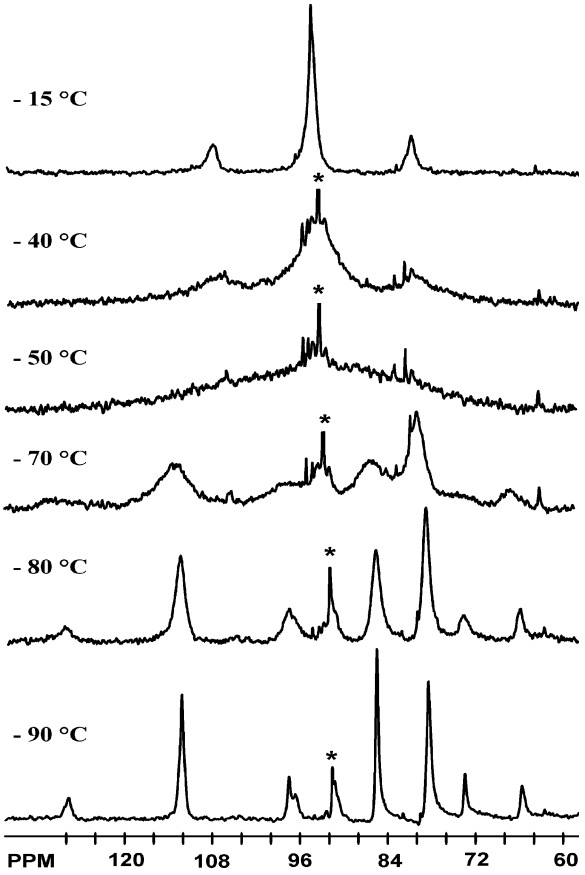

Figure 4. $^{31}P\{^1H\}$ NMR spectra at 202.5 MHz of compound **12** at various temperatures in toluene-d_8 solvent. Signal labeled with * is an impurity from $[Pt(PBu^t_3)]_3(\mu\text{-}CO)_3$.

increased steric interactions between the ligands. The metal cluster core is best described as an Rh_2Pt_2 tetrahedron with a $Pt(PBu^t_3)$ group bridging the Rh−Rh edge. The "unsaturation" present in compound **11** may have been shifted to the Pt2−Rh1 bond, which is considerably shorter in **12** than in **11**, 2.7821(10) vs 2.9521(7) Å.

The $^{31}P\{^1H\}$ NMR spectra of compound **12** at various temperatures are shown in Figure 4. At −90 °C the spectrum exhibits three resonances, $\delta = 112.2$, 85.5, and 78.5, all showing appropriate $^{31}P-^{195}Pt$ coupling, indicating that each of the phosphorus atoms are bonded directly to a platinum atom. This spectrum is completely consistent with that of the structure found in the solid state. However, as the temperature is raised, all three resonances begin to broaden and coalesce reversibly. Interestingly, it can be seen that two of the resonances at $\delta = 112.2$ and 85.5 broaden faster than the third resonance at $\delta = 78.5$ In fact, the resonances at $\delta = 112.2$ and 85.5 are exactly twice as broad as the resonance $\delta = 78.5$ at −80 °C. This broadening is indicative of dynamical exchange and the differences in broadening indicates that there are actually two different exchange processes occurring and the low-temperature process proceeds at a rate that is exactly twice the rate of the higher temperature process. Ultimately, all three resonances reform as a single averaged resonance at −15 °C. The ^{195}Pt satellites, $^1J_{^{31}P-^{195}Pt} = 5477$ Hz, observed at −15 °C is the average of the $^{31}P-^{195}Pt$ coupling of the three different phosphorus

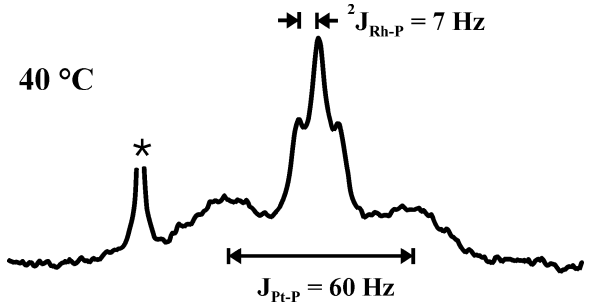

Figure 5. $^{31}P\{^1H\}$ NMR spectrum at 121.5 MHz of compound **12** at 40 °C in toluene-d_8 solvent, for the resonance at $\delta = 94.7$ at −15 °C in Figure 4. Signal labeled with * is an impurity from $[Pt(PBu^t_3)]_3(\mu\text{-}CO)_3$.

resonances at −90 °C. When the temperature was raised to 40 °C, fine structure was observed on the averaged resonance; see Figure 5. The fine structure consists of a triplet with a splitting of 7 Hz due to coupling to rhodium and broad Pt satellites due to multibond $^{31}P-^{195}Pt$ coupling, 60 Hz. The signal labeled with * in Figure 5 is an impurity identified as the compound $[Pt(PBu^t_3)]_3(\mu\text{-}CO)_3$ based on IR and NMR data in the literature.[19] The impurity is not involved in the exchange processes that are occurring for compound **12**.

The observation of one-bond $^{31}P-^{195}Pt$ and two-bond $^{31}P-^{103}Rh$ coupling in the average spectrum at 40 °C confirms that the rearrangement is an intramolecular process.[20] The exchange broadened spectra were simulated by line shape calculations by assuming a one-on-one exchange between the resonances at 112.2 and 85.5 ppm that proceeds at exactly twice the rate of their exchange with the resonance at 78.5 ppm. These rates have provided activation parameters in the usual way: $\Delta H^{\ddagger} = 8.2(2)$ kcal mol^{-1}, $\Delta S^{\ddagger} = -2(1)$ cal mol^{-1} K^{-1}, and $\Delta G_{258}{}^{\ddagger} = 8.7(5)$ kcal mol^{-1} for the lower energy process and $\Delta H^{\ddagger} = 8.2(3)$ kcal mol^{-1}, $\Delta S^{\ddagger} = -3(1)$ cal mol^{-1} K^{-1}, and $\Delta G_{258}{}^{\ddagger} = 8.9(6)$ kcal mol^{-1} for the higher energy process. Although the absolute values of the activation parameters for the two processes are technically equal within experimental error, it is also a fact that the differences between the activation parameters are true and more accurately known than the absolute values.

Proposed mechanisms for the interchange of the platinum atoms including the phosphine ligands attached to them in **12** are shown in Scheme 1. There are two possible ways to permute the Pt atoms without simultaneously averaging all three of them. These are represented by mechanisms **1** and **2**. By mechanism **1**, atoms Pt_2 and Pt_3 are averaged. Pt_1 remains unique. The process requires some accompanying shifts of some of the CO ligands and is not quite as simple as depicted in the schematic, but CO ligand migrations are generally facile in clusters such as these.[18] By mechanism **2**, atoms Pt_1 and Pt_2 are interchanged. Pt_3 remains unique. This mechanism requires two steps and involves a trigonal bipyramidal intermediate, such as found in the structure of **11**. The first step involves forming a bond between atoms

Scheme 1

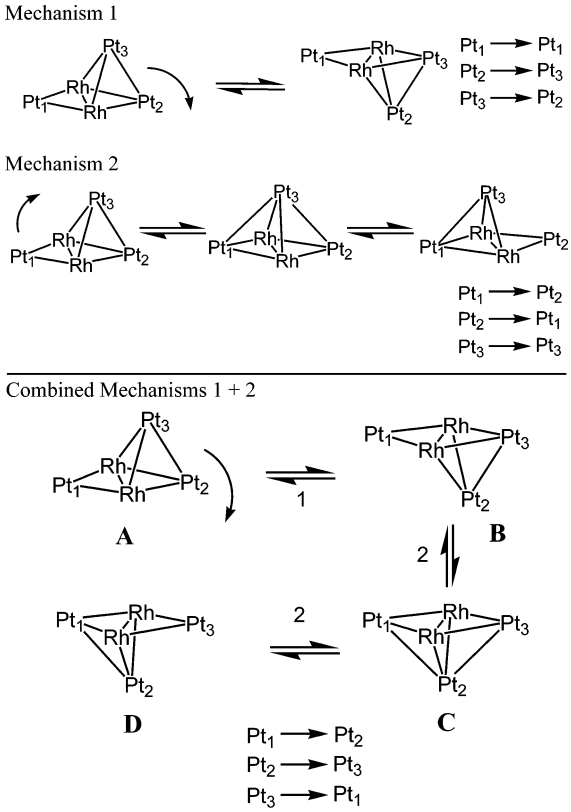

By combining the two mechanisms, all Pt atoms and their attached phosphine ligands are interchanged in the transformation of structure **A** to **D**.

Pt_1 and Pt_3 to produce a trigonal bipyramidal intermediate and then breaking a bond between Pt_2 and Pt_3. We cannot determine which of these two mechanisms is the more facile of the two. However, by combination of the two mechanisms, all the platinum atoms are averaged; see the representation "Combined Mechanisms 1 + 2" in Scheme 1. The structure of **12** is represented as **A**. By mechanism **1**, Pt_2 and Pt_3 are interchanged by transformation to **B**. By mechanism **2**, Pt_1 and Pt_3 are interchanged by transformation to **D** via the trigonal bipyramid intermediate **C**. The selective broadening visible in the low-temperature spectra is clearly indicative of two dynamic processes that are readily and rationally explained by the two mechanisms shown in Scheme 1.

When $Rh_4(CO)_{12}$ was treated with a large excess of $Pt(PBu^t_3)_2$ and heated to 68 °C, the hexarhodium−tetraplatinum cluster $Rh_6(CO)_{16}[Pt(PBu^t_3)]_4$, **13**, was obtained, but only in a very low 3% yield and the products **10**−**12** were not obtained. Compound **13** was characterized by a combination of IR, ^1H and ^{31}P NMR, and single-crystal X-ray diffraction analyses. An ORTEP diagram of the molecular structure of **13** is shown in Figure 6. Selected bond distances and angles are listed in Table 2. The compound consists of an octahedral cluster of six rhodium atoms. There are four $Pt(PBu^t_3)$ groups that have formed edge bridges on four Rh−Rh bonds. In the solid state the molecule has a crystallographic C_2 symmetry, but the symmetry of the Rh_6Pt_4 cluster is approximately D_{2d}, as can be seen in Figure 7. The molecule can be viewed as a tetra $Pt(PBu^t_3)$ adduct of $Rh_6(CO)_{16}$. There

(19) Goel, R. G.; Ogini, W. O.; Srivastava, R. C. *J. Organomet. Chem.* **1981**, *214*, 405.
(20) Jesson, J. P.; Muetterties, E. L. In *Dynamic Nuclear Magnetic Resonance Spectroscopy*; Jackman, L., Cotton F. A., Eds.; Academic Press: New York, 1975; Chapter 8.

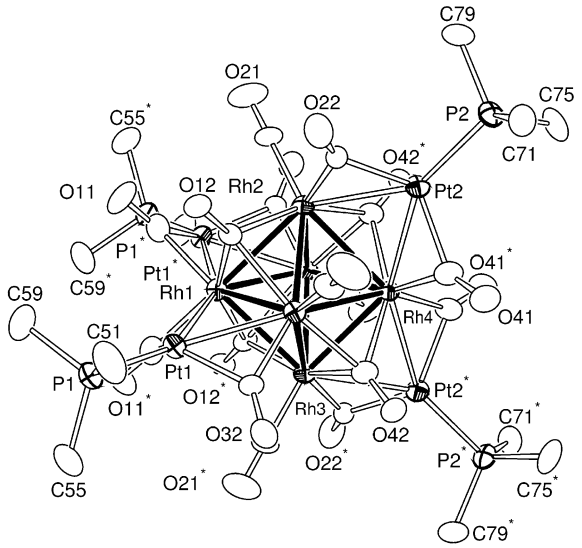

Figure 6. ORTEP diagram of the molecular structure of $Rh_6(CO)_{16}[Pt(PBu^t_3)]_4$, **13**, showing 30% probability thermal ellipsoids. The methyl groups have been omitted for clarity.

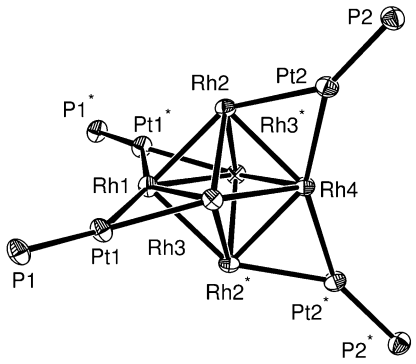

Figure 7. Diagram of the structure of **13** minus the carbonyl ligands and the *tert*-butyl groups of the phosphine ligands.

are four triply bridging CO ligands distributed about the Rh_6 core as found in the compound $Rh_6(CO)_{16}$.[21] By comparison, only two $Pt(PBu^t_3)$ groups could be added to $Ru_6(CO)_{17}(C)$ to yield the compound **2**.[9] Each of the Pt−Ru bonds in **13** has one bridging carbonyl ligand and there are only four terminal carbonyl ligands: one on each of the rhodium atoms Rh2, Rh2′, Rh3, and Rh3′. Atoms Rh(1) and Rh(4) have no terminal carbonyl ligands as both these atoms are bonded to two of the platinum atoms. The Rh−Rh bond distances lie in the range 2.7573(9)−2.8071(9) Å and are similar to those found in $Rh_6(CO)_{16}$.[21] The Rh−Pt bond distances lie in the range 2.7113(4)−2.7364(7) Å.

The $^{31}P\{^1H\}$ NMR spectrum of **13** shows large one-bond coupling to platinum ($^1J_{Pt-P} = 5977$ Hz) and a uniform 1:6:15:20:15:6:1 septet, indicative of equivalent coupling to all six rhodium atoms to the phosphorus atom, $J_{P-Rh} = 3$ Hz. However, as observed in the solid state, the rhodium atoms are not all magnetically equivalent in the structure of **13**. Thus, it seems that some dynamical averaging process may be operative in **13** that equilibrates the six rhodium atoms. The simplest process that could account for this is one that allows the $Pt(PBu^t_3)$ groups to migrate uniformly about the surface of the Rh_6 octahedron, similar to that observed in the compounds **6** and **7**.[11] Unfortunately, efforts to detect a slowing of the dynamical activity of **13** by ^{31}P NMR measurements at −80 °C were not successful.

In summary, the reaction of $Rh_4(CO)_{12}$ with $Pt(PBu^t_3)_2$ has yielded the tetrarhodium−platinum compound **10**, two dirhodium−platinum compounds **11** and **12** from Rh_2 fragmented species, and a hexarhodium−tetraplatinum compound **13** from Rh_6 condensed species. Fragmentation of the $Rh_4(CO)_{12}$ is evident from the formation of the dirhodium compounds **11** and **12**. Condensation of rhodium atoms is evident by formation of the higher nuclearity species **13**. These reorganizations are not unprecedented. For example, the reaction of $Rh_4(CO)_{12}$ with cyclohexa-1,3-diene yields the hexarhodium compound $Rh_6(CO)_{14}(\eta^4\text{-}C_6H_8)$.[22] Most interestingly, all of these compounds appear to exhibit dynamical activity involving ligand rearrangements and/or rearrangements of the metal atoms in the cluster itself. This work further demonstrates the ability of $Pt(PBu^t_3)$ groups to bind as bridging units across metal−metal bonds in polynuclear metal complexes. It seems that scope and variability of the $Pt(PBu^t_3)$ and $Pd(PBu^t_3)$ groupings in metal cluster chemistry appear to be large and should have major implications for future studies of the reactivity of these complexes toward small organic molecules in ligand substitution reactions and as substrates in catalytic processes.

Acknowledgment. This research was supported by the Office of Basic Energy Sciences of the U. S. Department of Energy under Grant No. DE-FG02-00ER14980. We thank Strem for donation of a sample of $Pt(PBu^t_3)_2$ and the USC Nanocenter for financial support.

Supporting Information Available: X-ray crystallographic data in CIF format are available for compounds **10**, **11**, **12**, and **13**. This material is available free of charge via the Internet at http://pubs.acs.org.

IC0353920

(21) (a) Farrar, D. H.; Grachova, E. V.; Lough, A.; Patirana, C.; Poë, A. J.; Tunik, S. P. *J. Chem. Soc., Dalton Trans.* **2001**, 2015. (b) Corey, E. R.; Dahl, L. F.; Beck, W. *J. Am. Chem. Soc.* **1965**, *85*, 1202.

(22) Dyson, P. J.; Ingham, S. L.; Johnson, B. F. G.; Blake, A. J. *J. Organomet. Chem.* **1995**, *498*, 237.